Lasers in Medical Science (2019) 34:1283–1293
https://doi.org/10.1007/s10103-019-02752-1

REVIEW ARTICLE

Polarization-resolved Stokes-Mueller imaging: a review of technology and applications

Spandana K. U.[1] · K. K. Mahato[1] · Nirmal Mazumder[1]

Received: 24 October 2018 / Accepted: 12 February 2019 / Published online: 4 March 2019

Abstract

Polarization microscopy, a powerful optical tool to study anisotropic properties of biomolecules, provides better microstructural information of a sample as compared with conventional optical microscopic techniques. The measurement and analysis of polarization states of light can be performed using both Jones matrix as well as Stokes algebra. Further, the details of optical properties of specimen are characterized by Mueller matrix. However, the application of Jones calculus is limited to perfectly polarized light, but Stokes-Mueller polarimetry is emerging as a promising tool for tissue imaging due to its application irrespective of polarization state of the light. In this review article, we explain the development of Stokes-Mueller formalism in context of linear optics. Furthermore, application of Mueller matrix decomposition (MMD) method to derive sample properties is demonstrated in several bio-medical studies.

Keywords Anisotropy · Optics · Microscopy · Polarimetry · Tissue · Imaging

Introduction

Optical polarization techniques are widely incorporated in imaging/microscopy with various light sources such as lamps, light emitting diodes (LED), and lasers [1–3]. The technique has several applications in the field of cellular and tissue imaging as well as material characterization [2, 4]. Compared with conventional optical microscopy techniques, polarization microscope provides additional microstructural information of biomedical specimens by revealing its optical anisotropic properties. The polarization microscope uses a polarizer before the sample to generate linear/circular/elliptical polarized light illumination and an analyzer placed after the sample, which is easy to implement but laborious for quantitative analysis [3–6]. Several research groups around the Globe are working on various modalities of polarization microscopy [4, 7, 8]. Shinya Inoue and Rudolf Oldenbourg at Marine Biological Laboratory, USA, have found remarkable improvement in an analytic power of traditional polarization microscope with an adoption of liquid crystal retarder, following quantitative birefringence distributions of mitotic spindle isolated from sea urchin eggs [4, 7].

To facilitate the treatment of complicated polarization problems at the amplitude level, R. Clark Jones developed a matrix calculus commonly called the Jones matrix calculus in early 1940s, in which polarized light is expressed by the complex quantities contained in 2×1 column matrices called Jones vector [9]. Several experimental techniques were developed based on Jones matrix for determining the birefringence properties of the sample [10]; however, Jones matrix formalism is restricted to fully polarized light which limits the various applications [9]. The complete state of polarization of light can be measured in terms of four Stokes polarization parameters; total optical field intensity was described by the first parameter and the polarization state was described by the remaining parameters. The Stokes parameters are a logical consequence of the wave theory and measurable quantities [9]. In 1985, a photo-polarimeter based on Stokes formalism was developed by R.M.A. Azzam to measure the complete polarization state of light simultaneously using four photo detectors [11]. Polarization property at the cellular level of living human eye was also measured by high-resolution Stokes imaging polarimeter [12]. Thereafter, four-channel photon counting based–Stokes polarimeter was designed to measure and analyze the state of polarization of second harmonic signal from non-centrosymmetric molecules (collagen fibers and starch granules) [13].

✉ Nirmal Mazumder
nirmaluva@gmail.com

[1] Department of Biophysics, School of Life Sciences, Manipal Academy of Higher Education, Manipal, Karnataka 576104, India

Stokes parameters describe the polarization properties of light; however, Stokes-Mueller formalism is suitable for detailed analysis of the sample. As a comprehensive explanation of sample's optical properties and structural information related to polarization, the Mueller matrix plays an important role in biomedical research and tissue characterizations [9]. The polarization signal depends on the orientation of molecules; hence, Mueller imaging shows significant enhancement of contrast from fibrous structures which is hardly seen under conventional polarization imaging. Yet, there exist lack of explicit association of Mueller matrix with microstructural properties and are critically affected by fibrous structure orientation. Several polarization effects occur simultaneously that cause "lumped" effect in Mueller matrix elements, thus hindering their unique interpretation; hence, the Mueller matrix of analyzed sample encloses its combined polarizing properties. To overcome this, 16 Mueller elements were transformed into sub-parameters with specific structural and physical properties. For example, Lu and Chipman proposed the Mueller matrix polar decomposition (MMPD) method, where the Mueller matrix was decomposed into a set of three basis matrices representing diattenuator, retarder, and depolarizer. These sub-matrices are converted into individual parameters associated to diattenuation, retardance, and depolarization properties [14, 15].

The theoretical development in the field along with the advancement in polarimetry has led to the promising performance of polarization microscopy [16, 17]. In recent days, polarization-based imaging techniques offer potential biomedical diagnosis for detection of anomalous tissues in the liver, skin, esophagus, cervix, colon, etc. [5, 8, 18]. High numerical aperture objective lens in optical microscopy causes polarization distortions in excitation as well as in the detection arms [19]. The polarization distortions from several components in the optical path were accounted with Stokes parameters [13]. Hence, to implement quantitative polarimetry, an imaging setup based on Stokes- Mueller formalism is important. By this way, spatially resolved polarization measurements allow detailed inspection of change in the sign and magnitude of the polarization parameters and also provide information regarding properties of the molecules.

Pathological diagnoses are time-consuming during the growth of cancer incidence. With precise observations using conventional transmission microscope, the pathologists need about half an hour to prepare the stained and frozen slices of peculiar tissue fragments from the patients. On the other hand, when polarization imaging technique is used, tissue features can be visualized to distinguish abnormal from normal without staining the specimens [8, 14]. In this method, sample's retardance as well as anisotropy is determined using birefringence properties of the scattered light from the sample whereas diattenuation and depolarization properties are determined using Lu-Chipman Mueller matrix [20, 21]. Furthermore, it was noticed that collagen-rich structures show high contrast with polarized light as a result of the birefringence features of the collagen fibers. Hence, the changes in tissue structures, particularly the collagen contents and organization, can be correlated with the tissue pathology using Stokes polarimetry module. Collagen production in cancer tissue could be identified and inspected by determining the degree of circular polarization (DOCP), linear polarization (DOLP), and angle of polarization (AOP) [8, 21, 22].

In a study, Hui Ma et al. demonstrated the characteristic features of multispectral transmitted Mueller matrix transformation parameters used to differentiate both normal as well as abnormal areas of thyroid and cervical cancerous tissues [23, 24]. It was found that for an unstained cancerous tissue, intrinsic anisotropic arrangements were remarkably highlighted in Mueller elements M34 and M24 associated to circularly polarized state of light. However, it was poorly enhanced for linear polarized state of light. In such circumstance, Mueller matrix measurement of the sample is useful in understanding the polarization property of the sample. As a non-stained technique, Stokes-Mueller matrix based microscope was aimed at developing and applying advanced polarization imaging methods to the elucidation of both frozen and standard pathological slices. This understanding may underlie the development of an effective treatment and therapy. R. Simon et al. have derived the necessary conditions for a real 4 × 4 Mueller matrix in linear systems. The derivations were then applied to experimentally measured results [25, 26]. R. P. Singh et al. are also working on the theoretical development of polarized light scatterings [27]. The main research on the development of Mueller polarimetry by his group is to study the interaction and coherence properties of lights through imaging in the future. P. K. Gupta and his team have developed polar decomposition method of Mueller matrix using nine element 3 × 3 Mueller matrix that involves only the linearly polarized light measurements [28]. The approach was based on Lu-Chipman decomposition method for 4 × 4 Mueller matrices with 16 elements [20]. The developed 3 × 3 polar decomposition was applied to turbid medium such as biological tissues and quantified the various polarization parameters including the circular retardance, linear retardance, linear diattenuation, and linear depolarization coefficient.

In this review article, we have incorporated mainly the Stokes-Mueller imaging techniques for biomedical applications. Accordingly, the inclusion criteria are polarization as well as Stokes-Mueller calculus methods, whereas Jones calculus has been excluded in this manuscript. We have used databases such as PubMed and Web of Science to gather information for this article. We discuss about applications of Mueller matrix decomposition method [29–36] to monitor changes in the infarcted myocardial tissue based on birefringence and also in non-invasive blood glucose measurements [30, 33]. Also, Mueller matrix microscopy and Monte Carlo

simulations were used to investigate the effect of structural changes in various stages of fibrosis in liver cancer on polarization parameters [32]. Further, multispectral Mueller matrix imaging studies were performed in ex vivo to stage colon cancer and to examine cancer persistence after treatment [31]. In a study, Mueller matrix images of collagen meshwork in articular cartilage were correlated with multiphoton microscopy [35]. Furthermore, we will be discussing on the application of Mueller imaging polarimeter in the colon, cervix tissue sample with both healthy and cancerous conditions [36–39].

Types of polarimetry: Stokes polarimeter and Mueller polarimeter

A Stokes polarimeter comprises of a light source, polarization state analyzer (PSA), and detector (I) [13]. Specifically, Stokes polarimeter of incoming signal is measured, as depicted by the associated Stokes vector, $S_{out} = [S_0, S_1, S_2, S_3]^t$. Each Stokes parameter can be rendered a physical significance [9] and provide critical as well as valuable information of the light through various polarization parameters including DOP, DOLP, and DOCP. For comparison, a Mueller polarimeter comprises of a light source, polarization state generator (PSG), sample, and PSA. The Mueller matrix, M describes how the polarization state of input light changes upon interaction with the sample by $S_{out} = MS_{in}$ where input Stokes vector "S_{in}" and the output Stokes vector "S_{out}". Full determination of the Mueller matrix is measured through sequential input of different polarization states, so that S_{out} and S_{in} be matrix quantities. Hence, Mueller matrix, $M = S_{out}\ S_{in}^{-1}$. Linear optical measurements widely incorporate Stokes-Mueller formalism [21, 24, 27] for investigating various polarization properties of the sample. The input and output polarization states of light are linked through Mueller matrix formalism by implementing Lu-Chipman decomposition [20, 21] and hence the analysis becomes a practical approach. Again, a full Mueller matrix formalism is limited to linear optics [20].

Mueller microscope

A commercial transmission light microscope (L2050, Liss Optical Instrument Factory, Guangzhou, China) can be upgraded to the Mueller matrix–based microscope by adding PSG and PSA to the existing optical path as shown in Fig. 1. The illuminating light from the LED (3 W, 632 nm, $\Delta\lambda =$ 20 nm) passes through a polarizer (P1, extinction ratio 500:1, Daheng Optics, China) and a rotatable quarter-waveplate (R1, Daheng Optics, China) of the PSG. The transmitted light after the sample is collected by an objective lens and passes through rotatable quarter-waveplate (R2, Daheng Optics, China) and polarizer (P2, extinction ratio 500:1, Daheng Optics, China) of PSA. The polarizers (P1, P2) were

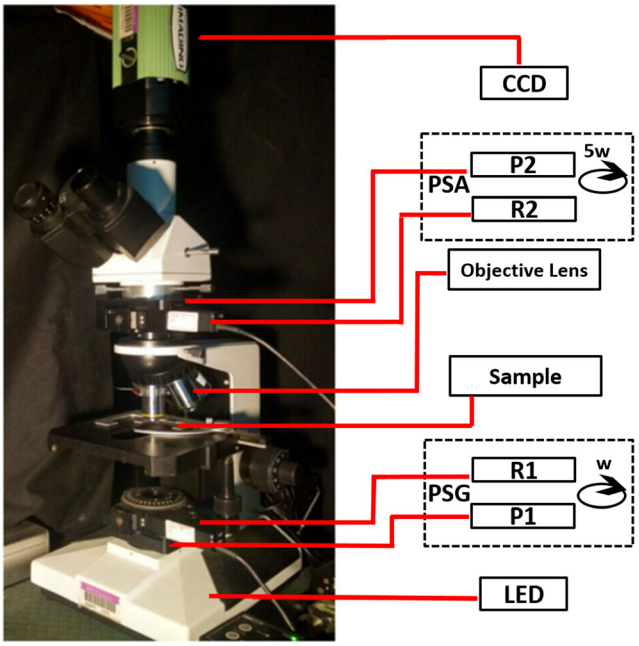

Fig. 1 Photograph and schematic representation of the Mueller matrix–based optical microscope. P1, P2—polarizer; R1, R2—quarter-waveplate; PSG—polarization state generator; PSA—polarization state analyzer. This figure is adapted with permission from ref. [34] OSA (BOE)

placed in the horizontal direction, while the retarders (R1, R2) have fixed rotation ($\omega 2 = 5\omega 1$) for each measurement. One of the advantages of LED is that it does not damage the tissue due to its non-coherent and non-collimating property. It generates broad band of wavelengths compared with single wavelength laser which affects wide range of tissue types and generates huge photochemical reactions. A compact module of PSG and PSA is designed and incorporated to the microscope. The polarization image of transmitted light is recorded by a 12-bit CCD camera (QImaging 74-0107A, Canada). The calibration of the microscope is performed by measuring the Mueller matrices of air, polarizer, and quarter-waveplate with about 1% error before applying to tissue samples. The system acquires 30 images for Mueller matrix reconstruction with specific characteristic combination in polarization states of incident and output light and Fourier coefficients are used to compute the obtained Mueller matrix elements [32, 34].

Applications of Stokes-Mueller imaging

At present, optical polarimetry is acquiring appreciable attention as a diagnostic tool in medical field, as it provides additional information when compared with traditional intensity-based measurements. Polarimetric imaging is favorable for biomedical applications for various reasons: (i) it characterizes the morphological changes in the tissue structure by exploiting polarization property of light; (ii) wide field images

(up to 20 cm^2) are produced for the analysis of large region of interest in specimen; (iii) being a non-invasive technique, it acquires tissue images without any contact and external labeling; (iv) it can be designed using inexpensive white light sources such as halogen lamps or LEDs which are harmless for samples and to patients at an optimal energy. Recent findings have shown the immense potential of polarimetric-based optical imaging in detection of pathological regions on an outstanding variety of tissues [30] such as the intestine [40], skin [18], and colon [8, 31, 36, 37, 41]. There are several groups working on the development of Stokes-Mueller polarimetry which has extensively been applied to numerous biomedical problems [13, 21, 23, 24, 31, 34, 35, 38].

Mueller imaging of myocardium and cartilage tissue

Cardiovascular disease due to myocardial infarction has led to the death of around 7.5 million people in a year [21]. Myocardial infarction results in the loss of cardio myocytes due to necrosis and rise in collagen with scar formation; however, stem cell–treated regenerative therapy found to improve the cardiac function. Most of the thick tissue samples cause extensive depolarization due to the multiple scattering; hence, a method was needed in order to account for it and to extract the individual contributions of simultaneously occurring polarization effects. Mueller matrix decomposition methodology was used to derive the individual polarization properties in scattering media [21].

In a study, the structural anisotropy of heart tissue was characterized by employing birefringence measurements to differentiate between regions of healthy, infarcted as well as regenerating myocardium. Changes in birefringence attributed to infarction of myocardium and stem cell regenerative treatments measured in rat model showed the efficacy of the method to track regenerative treatments [21, 30]. The heart samples were obtained in an established model in which myocardial infarction was induced in Lewis rats through coronary artery ligation. Mesenchymal stem cells transfected with human elastin gene were administered to the treatment group by intra myocardial injection at the site of infarction 2 weeks after the ligation procedure. Stokes-Mueller polarimetry was used to measure the normalized Stokes parameters of the light and Mueller matrices of the sample. The measured Mueller matrix was decomposed into three basis Lu-Chipman matrices to quantify simultaneously occurring effects such as depolarization, optical activity, and birefringence separately. Validity of this approach has been demonstrated theoretically by Monte Carlo simulation method and practically by tissue simulating phantoms. Second harmonic generation (SHG) and two-photon-excited fluorescence (TPEF) microscopy were performed on cardiac samples to image extracellular collagen matrix and on cardiomyocytes, respectively. This approach revealed useful information regarding microstructure and composition of tissue including infarction and regeneration process. Mueller matrix point measurements exhibit retardance value of 1.4 rad in healthy regions of myocardial tissue which corresponds to a birefringence value $\Delta n \leq 1.4 \leq 10^{-4}$. And infarcted regions exhibit large reduction in retardance value which indicates loss of tissue anisotropy; the marginal regions showed reduced retardance but not as low as the infarcted region (Fig. 2). These findings were confirmed by histology as well as multiphoton microscopy. Regenerative treatments found to increase the tissue anisotropy by remodeling scar tissue which led to improvement of cardiac function.

Osteoarthritis is a disease characterized by structural changes in articular cartilage, with symptoms of reduced joint function and pain. It can be diagnosed with radiographic and magnetic resonance imaging (MRI) but the association between the findings is not strong. Whereas bright-field light microscope could assess the microscopic structure of cartilage and the qualitative information on the direction of collagen fibers were examined by traditional polarization microscope and second harmonic generation (SHG) microscopy [35]. Morten Kildemo et al. utilized a near-infrared Mueller matrix imaging ellipsometer to characterize the degree of orientation of the collagen fibers from the intermediate layer of articular cartilage [35]. Mueller matrix imaging (MMI) extracts full Mueller matrices for every pixel in the image of both complex and unexplored sample. SHG technique lags behind MMI in faster scanning and resolving collagen fibers below the diffraction limit. However, integration of both techniques imparts a useful insight of osteoarthritis. MMI images were acquired from the medial femoral condyle of chicken cartilage sample and were decomposed using forward polar decomposition method which enables the measurement of birefringence, optical rotation, depolarization index, and the direction of slow axis. Retardance and depolarization images as shown in Fig. 3 revealed the resemblance in the areas with higher retardance as well as higher depolarization index due to higher concentration and larger size of collagen fibers. Thus, SHG microscope integrated with MMI plays an important role in the diagnosis which makes it significant for better assessment of the diseased cartilage structure in histopathology studies [35]. The detailed birefringence properties of collagen fibers of tendon tissue were obtained in the 3-D directional images from the acquired transmission Mueller matrix images (MMI)s at various angle of incidence [26].

Mueller imaging for tissue characterization in in vivo

In-vivo Mueller imaging was demonstrated to investigate the changes in tissue structure using a dorsal skinfold window chamber in a mouse model [33]. The Mueller polarimeter system employed photoelastic modulator (IS-90, Hinds

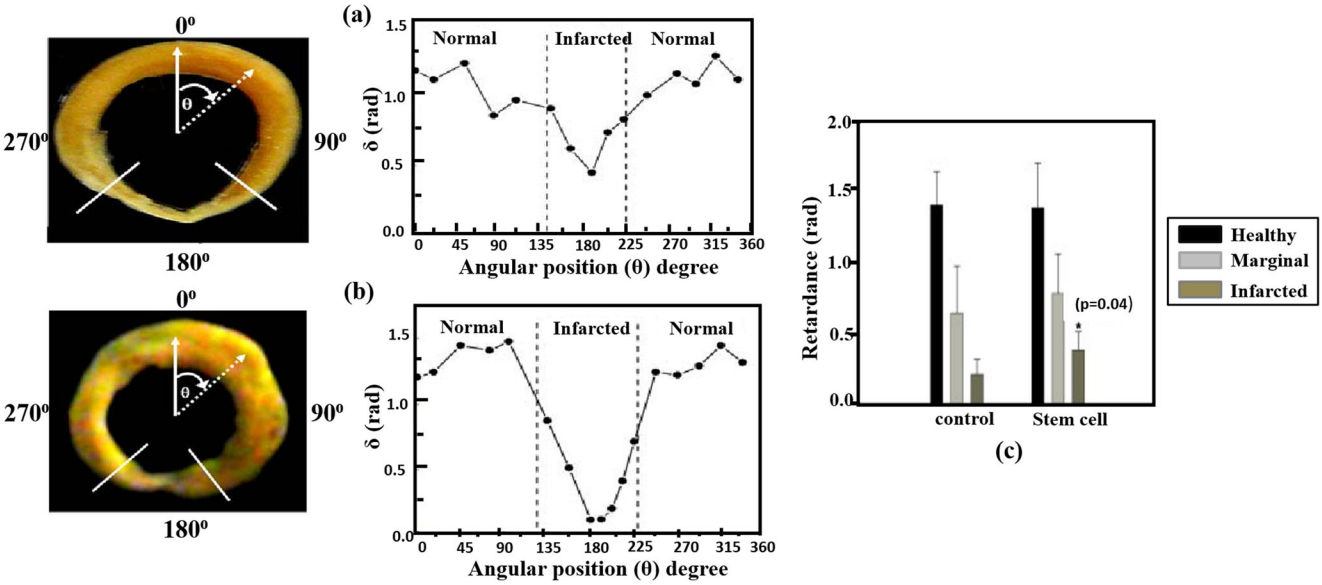

Fig. 2 Linear retardance measurements in 1-mm-thick tissue sections. (a) Untreated and (b) stem cell–treated tissues. The area marked around $\theta = 180°$ represents the infracted region. Birefringence values are decreased in the infarcted region compared with normal. The difference is reduced upon stem cell treatment as retardance values also increased in normal regions. This figure is adapted with permission from ref. [30] Wiley (J. Biophotonics). (c) Mean retardance pixel values measured by point measurement for control ($n = 4$), marginal, and stem cell–treated ($n = 3$) animals; error bars represent standard deviation. * represents statistical significance ($p = 0.05$) with respect to control. This figure is adapted with permission from ref. [21] SPIE (JBO)

Instruments, Hillsboro, OR) and synchronous lock-in detector (SR830, Stanford Research Systems, Sunnyvale, CA) for Stokes vector measurements as shown in Fig. 4. Ten-millimeter diameter of the dorsal surface region from the inner skin layer of an athymic nude mouse (NCRNU-M, Taconic, Hudson, New York) was removed and skin flap was held vertically by suturing titanium saddle; a tissue plane was covered with glass coverslip of thickness 145 ± 15 μm. Five microliters of collagenase was microinjected into the tissue region to induce the changes in the skin. Laser beam of 1 mm diameter from He-Ne source (λ=632.8 nm) was allowed to pass through the sample. By various combinations of the input polarization state as well as output Stokes vectors using a waveplates and linear polarizer, the Mueller matrix (M) was measured from distant control and collagenase-injected region. Using polar decomposition method, the birefringence and depolarization values calculated and plotted as a function of time in the control and collagenase-treated regions. For collagenase-treated region, retardance values range from $\delta =$ 1.2 rad to $\delta = 0.3$ rad; however, for the control region, values remain constant at $\delta = 1$ rad with treatment time. The small fluctuation in the control-tissue values indicates the

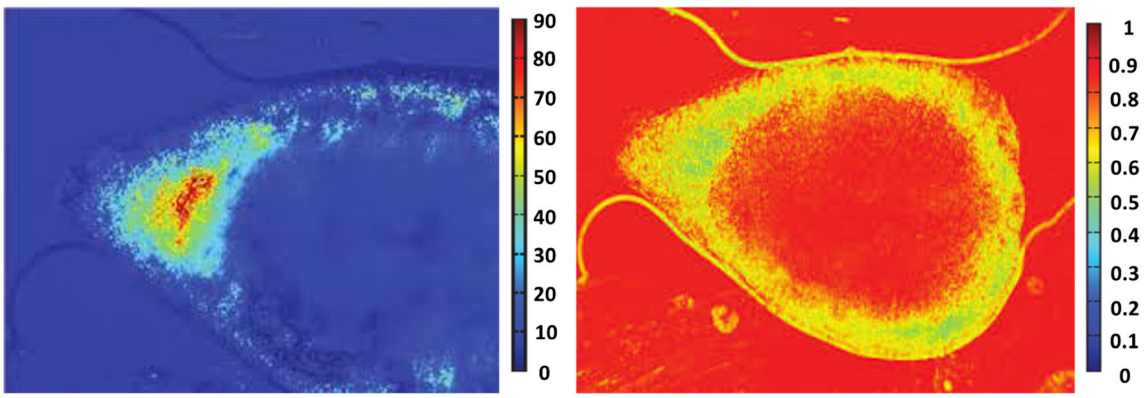

Fig. 3 (a) Retardance and (b) depolarization index images of cartilage tissue. The absolute linear retardance values represented as color bar in degree. The depolarization values range from 0 to 1; 1 is fully polarized and 0 is fully depolarized. This figure is adapted with permission from ref. [35] SPIE (JBO)

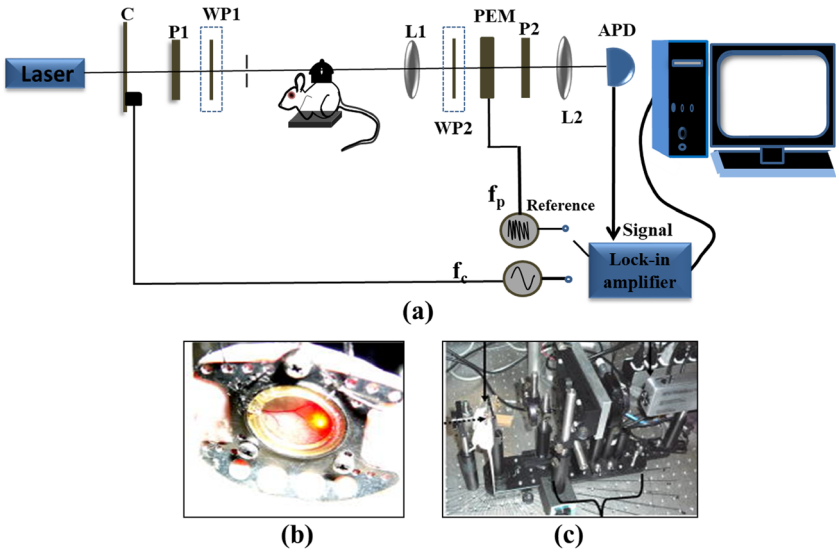

Fig. 4 (a) Schematic representation of the Mueller matrix measurements system in vivo: C: mechanical chopper; P1 and P2: linear polarizers; WP1 and WP2: quarter-waveplates; L1 and L2: lenses; PEM: photoelastic modulator; APD: avalanche photodiode; fc and fp: modulation frequencies of mechanical chopper and PEM, respectively. (b) Photograph of the dorsal skin flap window chamber model in a mouse. (c) Photograph of the experimental setup, showing implanted window chamber of mouse in the path of the beam. This figure is adapted with permission from ref. [33] SPIE (JBO)

reproducibility of the measurements over time. The reduction in birefringence was mainly due to denaturation of collagen fiber which also reduces the structural anisotropy. This method could accurately quantify tissue parameters such as birefringence and scattering and is expected to have applications in tissue diagnosis and for monitoring response after the treatment [33].

Mueller matrix imaging for cancer diagnosis and staging

Over the years, cancer is one of the major threats to human health, with liver cancer in the top five in both occurrence and mortality rate. During liver cancer development, tissues undergo cirrhosis due to fibrosis, a process of healing in response to liver damage. In a study, samples from fibrotic liver tissue in different stages were detected using a Mueller matrix microscope and analyzed using Mueller matrix transformation (MMT) as well as Mueller matrix polar decomposition (MMPD) methods. The scorings of pathological tissue samples were also quantitatively facilitated from cirrhosis to cancer. Four slices of 8-μm-thick human liver tissues in various fibrosis stages (F1 to F4) were used under investigation.

The increased values of parameters δ and t from F1 to F4 stage result in prominent retardance effect. However, there was a significant change in the mean value of δ when compared with t, showing that δ is sensitive to fibrous structure variation as shown in Fig. 5. Sphere birefringence model based on Monte Carlo (MC) simulations was conducted to examine the impact of structural variation in distinct fibrosis stages on the imaging parameters. The parameters δ of MMPD and t of MMT indicate retardance of the media, whereas the parameters θ of MMPD and x of MMT relate to the direction of fibrous structure orientation. Thus, fibrous liver tissues can be detected using deduced parameters such as δ, t, θ, and x. The experimental and MC-simulated results show the potential of polarization-based Mueller matrix microscope to deduce quantitative information related to pathological variations of liver tissues in several fibrosis stages [32].

Biopsy has been the gold standard for cancer diagnosis which refers to the removal of a tissue sample from a living subject, followed by the analysis of thin slices of extracted tissue under the microscope. Ex vivo multispectral Mueller polarization imaging was expected to stage colon cancer in human and to deduce the effectiveness of treatment in a short period of time [8, 36, 37]. Compared with the unpolarized intensity images, polarized backscattered light provides better image contrast with essential information about the tumor properties. Various polarization parameters such as depolarizing power, diattenuation, and retardance are deduced from Mueller matrix using Mueller matrix decomposition. Sixteen raw images were acquired from human colon specimens including both healthy and cancerous regions with various composition of input as well as output states of polarization at discrete wavelength using wide field Mueller imaging. Diagonal Mueller matrices in Fig. 6 indicate that colon tissue does not exhibit either retardance or diattenuation, therefore acting as partial depolarizer. The relation $|M22| = |M33| > |M44|$ holds true for both healthy and cancerous tissues showing that when compared with circularly polarized incident light, linearly polarized light exhibits reduced depolarization for back scattered light (as shown in Fig. 6). Measurements were performed within 500–700 nm light wavelength which is much shorter than the diameter of cell nuclei. It was demonstrated that at short wavelengths, both earlier and ulcerated cancerous areas depolarize less than healthy tissue.

Ex vivo human colon cancer specimens revealed enhanced contrast between healthy region and cancerous section. The

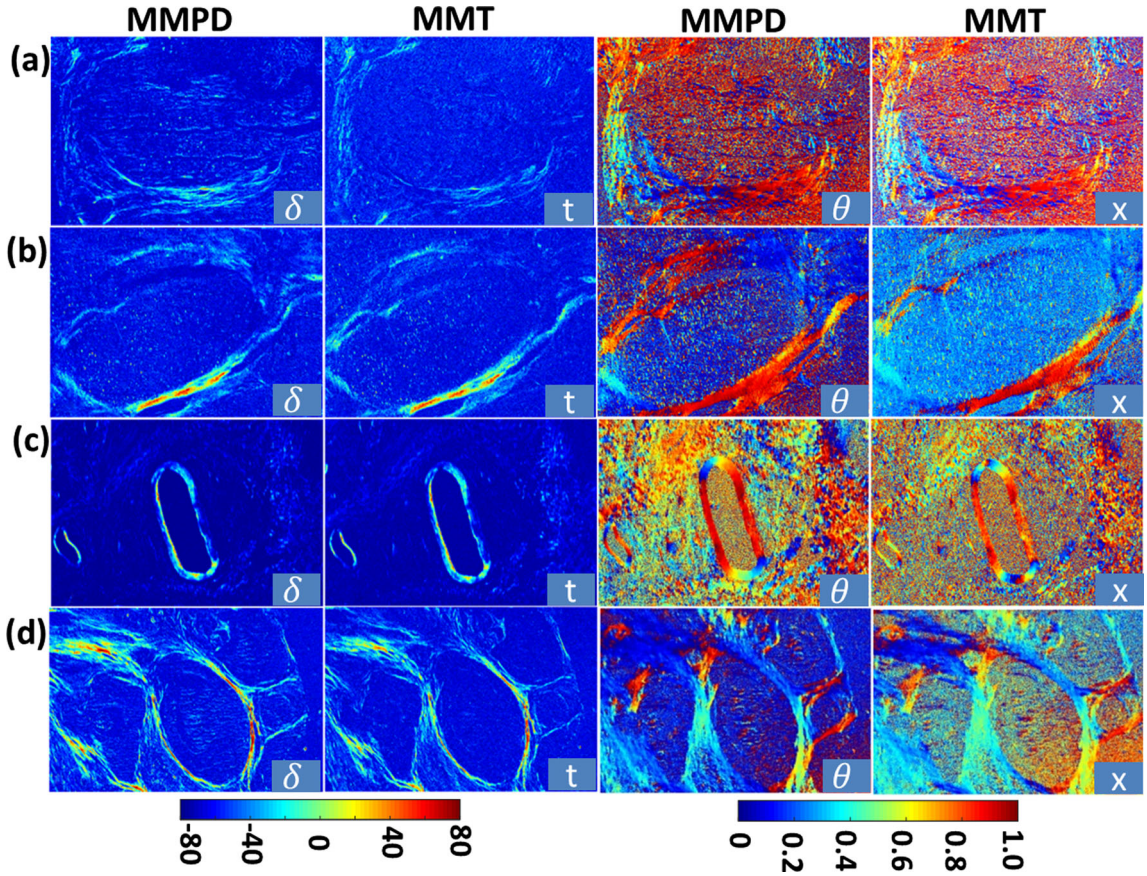

Fig. 5 Images of MMPD (δ, θ) and MMT (t, x) for 8-μm-thick non-stained dewaxed human liver tissue with fibrosis at (a) F1 stage, (b) F2 stage, (c) F3 stage, (d) F4 stage. This figure is adapted with permission from ref. [32] SPIE (JBO)

level of depolarization is not homogeneous within the ulcerated region. Cancerous tissue with high vascularization and high cellular density depolarizes less than the other tissues. The measured depolarization also depends on the tissue thickness, direction of projection, and light penetration depth in the colon layer [8]. Backscattering Mueller matrix images provide useful contrasts for healthy as well as cancerous regions of colon samples. The experimental results were interpreted by Monte Carlo modeling as well. At the early stage of the cancer, tumor regions are found to be less depolarizing than the healthy tissue as shown in Fig. 6c. It is observed that M_{22} and M_{33} images are identical for linearly polarized incident light, meaning that depolarization of backscattering was independent of polarization plane orientation. The absolute values of

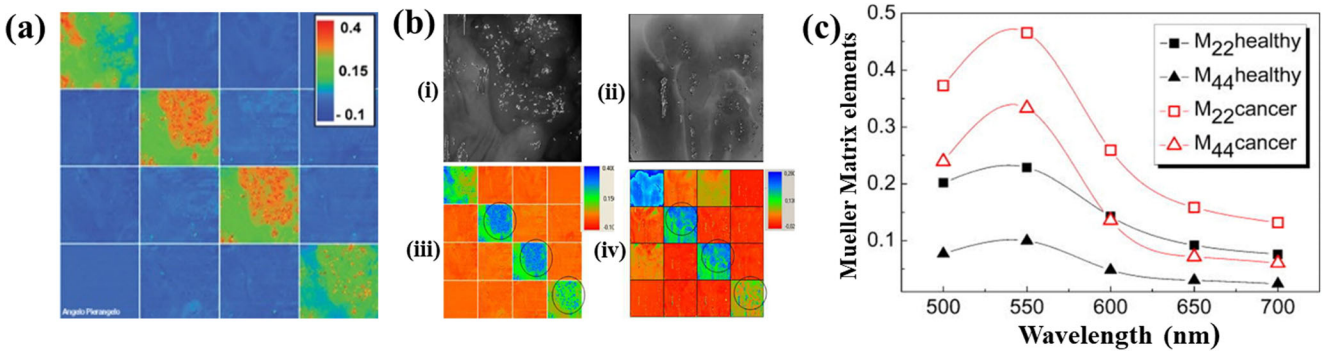

Fig. 6 (a) 16 Mueller matrix images of cancerous polyp acquired at wavelength of 600 nm. Each element of polarimetric images was normalized by the corresponding pixel value of the M11 image. This figure is adapted with permission from ref. [8] OSA (OPN). (b) Photo of a colon sample and with a tumor in the upper right part of the image was taken at (i) 600 nm, (ii) 700 nm, (iii) the reconstructed normalized Mueller images of the samples (i) at 600 nm, (iv) of (ii) at 700 nm. This figure is adapted with permission from ref. [37] OSA (OE). (c) Compares the experimental spectral dependence of diagonal elements M22 (square) and M44 (triangle) averaged over healthy (black) and cancerous (red) regions of colon sample. This figure is adapted with permission from ref. [36] of AIP publication

M_{22}, M_{33}, and M_{44} are higher on the diseased tissue than in healthy regions, which suggest a lower depolarizing power. Twenty healthy and cancerous colon tissues samples were used for polarimetric images where contrast arises due to light scattering from small scatterers and absorption of light by hemoglobin. M_{22} and M_{44} values decrease with increase in wavelengths since blood hemoglobin absorbance decreases.

For light propagating in multi-layered scattering medium, a numerical Monte Carlo model was proposed and further it was validated with the experimental results on tissue phantoms. Optical contrast from both healthy and cancerous region of colon tissue was also simulated between the scatterers and the surrounding medium for biological tissues. Nuclei and cytoplasm of the cells in tissues express polarimetric contrasts due to the low refractive index between them [37]. These results reveal that multi-spectral Mueller imaging provides image contrast enhancement for detection and staging of colon cancer ex vivo and to differentiate among histological variants of tumor. The work paves the way for the biomedical applications in in vivo Mueller matrix imaging. In addition, the technique provides quick and accurate significant clinical information, expected to be a promising tool in medical cancer care [36].

On the other hand, it is known that ultra violet radiation (UVR) is injurious to human skin tissue and lead to skin aging and cancer. Skin tissue consists of elastin and collagen fibers and is damaged when exposed to UVR. Polarization properties of light are sensitive to structure of the tissues. In this regard, changes in elastic fibers and collagen of nude mouse skin were detected by Mueller matrix polarimetry and demonstrate a quantitative, noncontact technique for monitoring the microstructural changes of skin tissues during self-repairing processes as well as UVR-induced photodamage [42]. Polarization parameters were found to be potential indicators of fibrous microstructure in skin tissues when compared with skin samples with and without sunscreen application. Microscopic analysis of the skin tissues from HE-stained slices of nude mouse and Monte Carlo simulations were correlated with the extracted Mueller matrix parameters from fibrous structures. Thus, the Mueller matrix–based technique paves the way for non-contact evaluation of skin structure in cosmetics and dermatological health.

Cervical cancer is the second most common cancer among females worldwide [43] and it was shown that accuracy of screening is significantly improved by Mueller imaging polarimetry [38, 44]. The anisotropy value of healthy tissues was strong in ex vivo fresh cervical specimens compared with the presence of pre-cancerous lesions [38]. Mueller polarimetric imaging was used to evaluate the anisotropy properties quantitatively from 17 fixed cervical samples. The sensitivity and specificity of tissue anisotropy quantification differentiate healthy squamous epithelium and high-grade cervical dysplasia. The anisotropy value in healthy squamous epithelium and pre-cancerous evolution was represented by the signature of the structure of collagen fibers [44]. The higher value of anisotropy represents the ordered and structured collagen in healthy squamous epithelium; however, pre-cancerous collagen fibers surrounded by connective tissue are degraded by the epithelium [45].

A case study of polarimetric-based macroscopic imaging of healthy and anomalous cervical samples both in ex vivo and in vivo was performed with 550 and 700 nm wavelengths [38]. Mueller decomposition method was applied to the acquired Mueller matrix for retrieving the polarimetric properties of the samples. Four ex vivo cervical tissue samples have been investigated and the results were characterized in detail by standard pathology (Fig. 7). Out of four, one was healthy, another carried Cervical Intraepithelial Neoplasia (CIN) lesions at very initial stage (CIN1) in its visible exocervical region, and the remaining two had advanced (CIN3) lesions with visible glandular epithelium (ectropion). In the healthy regions of both in vivo and ex vivo samples, significant birefringence was observed. In healthy regions, retardation and depolarization power was strong and in the anomalous regions of the other three ex vivo samples, they disappeared. The second sample clearly showed that retardance was strongly reduced in the central part. In the third sample, healthy region exhibited strong depolarization and retardation. In contrast, retardation reduced to a very small value in both CIN3 and glandular parts. Since, colposcopy being a notoriously difficult and operator-dependent technique, polarimetric imaging could be a possible alternative in this respect.

Mueller matrix polarimetry for optical clearing tissue

In human, 30 to 40% of total body weight constitutes of skeletal muscle tissues, with myofibrils as a basic component of muscle fibers. Microstructural variations in myofibrils can be associated to abnormal/disease condition of skeletal muscle tissues. Mueller matrix images in backscattering geometry were obtained with microstructural probing of bovine skeletal muscle tissues. Frequency distribution histograms (FDHs), 2D backscattering Mueller images, and Mueller matrix transformation (MMT) technique were combined to analyze tissue features in various physiological status [46]. Mueller matrix imaging along with Monte Carlo simulation acts as a powerful tool for investigating microstructural features of biological tissues.

In another study, backscattering Mueller matrices were acquired from nude mouse skin with immersion in glycerol solution. Mueller matrix elements with the various immersion time were compared and found that the M_{22}, M_{33}, M_{34}, M_{43}, and M_{44} values are sensitive to the time. A sphere-cylinder birefringence model (SCBM) of the skin was set to attain a deeper understanding on how the skin microstructures vary during the tissue optical clearing (TOC). Monte Carlo simulations were performed using scattering models which

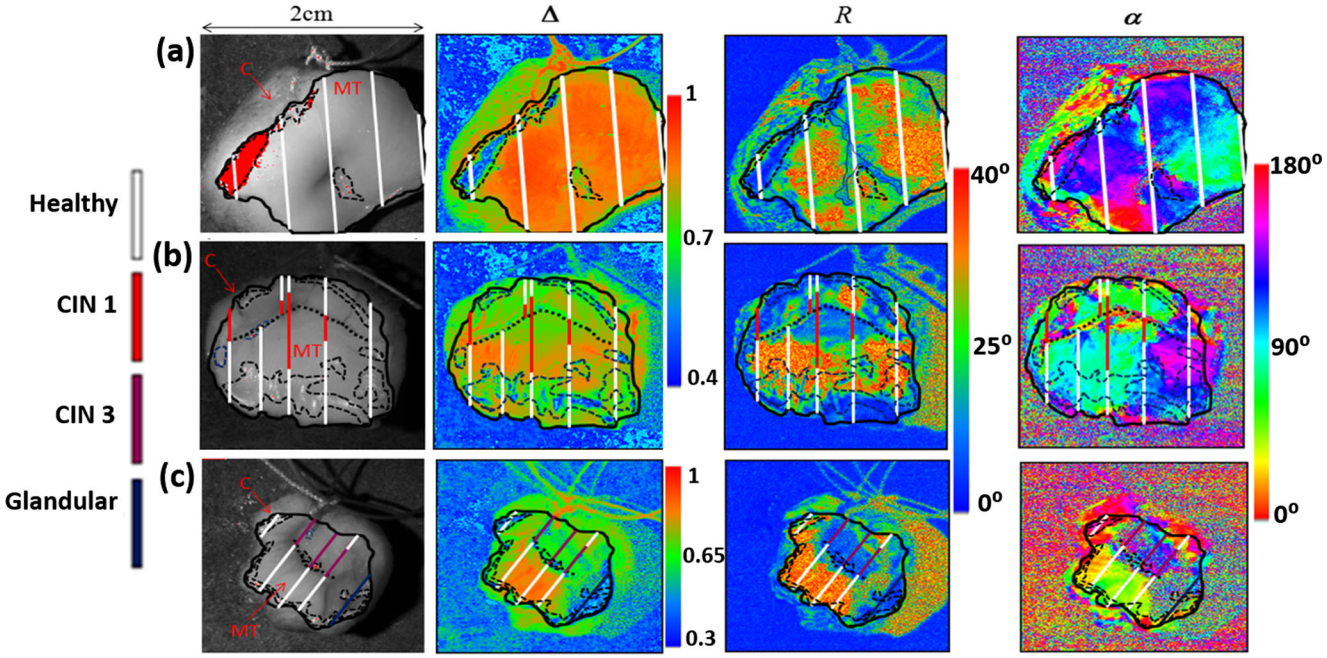

Fig. 7 Polarimetric images. (a) A healthy cervix sample with white lines representing histological cuts, taken at 550 nm. Inside the image, the limits of the cut are shown by black solid line, with stroma (C) outside and malpighian tissue (MT) inside. Followed by images of depolarization Δ, scalar retardation R (in degrees), and birefringence orientation α; (b) CIN1 and healthy tissue exhibited by conization specimen, endocervix orifice is indicated by dotted line inside the image; (c) CIN3, healthy tissue and glandular tissue. This figure is adapted with permission from ref. [38] OSA (OE)

correspond to different TOC mechanisms. TOC improves the penetration depth, contrast of image, and demonstrates its potential application in diagnosis. From the experimental results, it was found that with immersion time, the magnitude of diagonal Mueller matrix elements M_{22}, M_{33}, and M_{44} increased which reveals the reduction in the sample's depolarizing ability. The increasing absolute values of M_{34}, M_{43}, M_{12}, and M_{21} reflect scattering, induce anisotropies, and increase in birefringence. The absolute values and variations of M_{34} and M_{43} were much larger than those of M_{12} and M_{21} disclosing that the interstitial birefringence dominated skin anisotropy [47].

Discussion

Polarization imaging, mainly Mueller polarimetry, has various unique advantages as in situ and non-contact technique for identifying tissue microstructures [30, 48]. Stokes-Mueller polarimetry enhances the image contrast in superficial layers and is compatible with other optical systems too [31, 49]. A set of quantitative parameters with specific physical meaning have been acquired from 16 elements of Mueller matrix [20]. Furthermore, comprehensive characterization of the polarization properties of the sample using the Mueller matrix is found to have increasing application in textile samples of various microstructures such as cotton, acetate, ramie, and silk [15]. Classic colposcope had been used for screening cervical cancer; however, it suffers lack of contrast and magnification. Whereas, Mueller imaging facilitates the detection as well as quantification of variations of the collagen fibers due to the growth of a precancerous lesion in the uterine cervix [38, 39]. A wide field Mueller Polarimetric Colposcope (MPC) was constructed by inserting a miniaturized Mueller polarimeter for an in vivo study of uterine cervix which examined a number of patients in the field. The advantage of the new imaging tool is its compactness, performs fast image acquisition, hassle-free handling for a specialist with little modifications to their existing practice, and eliminates any distorting effects due to movement of patients [39]. A spectroscopic Mueller matrix technique was also developed to explore polarization properties of fluorescence signal from biological tissues. This Mueller matrix measurement explored the spectroscopic signature of polarimetric studies on normal and precancerous tissue fragments from human uterine cervix [28].

Mueller matrix polarimetry as a noncontact approach has shown its potential to monitor changes in microstructures of skin tissues due to photodamage induced by ultraviolet rays, hence, serve as quantitative and low-cost technique which is beneficial in the field of dermatological health as well as cosmetics [42]. Also, combination of Mueller matrix imaging with Monte Carlo simulation exhibits several clinical applications by connecting tissue microstructure with its respective polarization optical properties [47]. Multi-spectral Mueller imaging could be useful in verifying the residual cancer presence in Radio chemotherapy–treated colon samples. Even though the technique cannot replace classical histology, it can significantly improve the

comprehensive performance of pathologist [41]. In this regard, Mueller matrix–based applications in pathological tissues, such as cervical cancer [38, 39], colon cancer [41], liver fibrosis [32, 36, 37], and skin cancer [18, 42, 47], have shown the potential of the Mueller matrix parameters in diagnosis. The quantitative information is also obtained using decomposition of Mueller matrix into three basis matrices, namely, diattenuation matrix, retardance matrix, and depolarization matrix based on polar decomposition method. The approach was validated and analyzed in chiral and birefringent turbid media such as biological tissues [30]. Eventually, Stokes-Mueller polarimetry has paved the way for a variety of robust, noninvasive techniques for several biomedical applications.

Conclusion

Several research groups are working on the development of non-linear polarization imaging using Stokes-Mueller formalism. Two-channel-based polarization-resolved second harmonic generation (SHG) microscopy demonstrated that it can determine orientation of collagen fibers in different tissues [50]. Further, four-channel-based Stokes polarimeter was developed and implemented in SHG microscopy to characterize the polarization state of SH light from collagen fibers and starch [13]. However, the technique is limited to characterize the linear light and not applicable for non-linear light which need to explore more. Also, Mueller matrix ellipsometer (MME) was designed based on near-infrared (NIR) ferroelectric liquid crystal (FLC) and was demonstrated in birefringence imaging of strain in multi-crystalline silicon wafers. Material costs for the silicon solar cell can be reduced by achieving the lower wafer thickness; however, reducing the wafer thickness was hindered by internal residual strain. The polarimetric information of the wafer was extracted from a Mueller matrix measured based on forward polar decomposition techniques. The system has been proven to be a potential tool in the characterization of strain in NIR transparent solids and multi-crystalline silicon [49]. Polarimetry deals with the interaction of polarized light with materials and characterizes the structural properties of biological tissue through the changes in linear birefringence. Although, due to the high scattering nature of tissues, depolarization occurs and will eventually lead to the loss of signal information. Polarimeter methods have several advantages over other traditional optical imaging modalities such as being more sensitive to larger sampling depths, less complex, and less expensive.

Acknowledgements We thank SERB-Department of Science and Technology (DST), Government of India for financial support. The authors thank Dr. K. Satyamoorthy, Director, School of Life Sciences, MAHE, for his encouragement and Manipal Academy of Higher Education, Manipal, for providing the infrastructure and facilities.

Funding information This study was financially supported by SERB-DST, Government of India (Project Number—ECR/2016/001944).

Compliance with ethical standards

Conflict of interest The authors declare that they have no conflict of interest.

References

1. Schoenenberger K, Colston BW, Maitland DJ, Da Silva LB, Everett MJ (1998) Mapping of birefringence and thermal damage in tissue by use of polarization-sensitive optical coherence tomography. Appl Opt 37(25):6026–6036
2. Mockaitis K, Estelle M (2008) Auxin receptors and plant development: a new signaling paradigm. Annu Rev Cell Dev Biol 24:55–80
3. Kliger DS, Lewis JW (2012) Polarized light in optics and spectroscopy. Elsevier, Amsterdam
4. Oldenbourg R, Mei G (1995) New polarized light microscope with precision universal compensator. J Microsc 180(2):140–147
5. Tuchin VV (2016) Polarized light interaction with tissues. J Biomed Opt 21(7):071114
6. Shindo Y, Oda Y (1992) Mueller matrix approach to fluorescence spectroscopy. Part I: Mueller matrix expressions for fluorescent samples and their application to problems of circularly polarized emission spectroscopy. Appl Spectrosc 46(8):1251–1259
7. Inoué S (2008) Microtubule dynamics in cell division: exploring living cells with polarized light microscopy. Annu Rev Cell Dev Biol 24:1–28
8. Novikova T, Pierangelo A, De Martino A, Benali A, Validire P (2012) Polarimetric imaging for cancer diagnosis and staging. Opt Photonics News 23(10):26–33
9. Hecht E (2002) Optics, 4th International edn. Addison-Wesley, San Francisco 3:2
10. Brasselet S (2011) Polarization-resolved nonlinear microscopy: application to structural molecular and biological imaging. Adv Opt Photon 3(3):205
11. Azzam R (1985) Arrangement of four photodetectors for measuring the state of polarization of light. Opt Lett 10(7):309–311
12. Song H, Zhao Y, Qi X, Chui YT, Burns SA (2008) Stokes vector analysis of adaptive optics images of the retina. Opt Lett 33(2):137–139
13. Mazumder N, Qiu J, Foreman MR, Romero CM, Török P, Kao F-J (2013) Stokes vector based polarization resolved second harmonic microscopy of starch granules. Biomed Opt Express 4(4):538–547
14. Ghosh N, Wood MF, Vitkin IA (2008) Mueller matrix decomposition for extraction of individual polarization parameters from complex turbid media exhibiting multiple scattering, optical activity, and linear birefringence. J Biomed Opt 13(4):044036
15. Sun M, He H, Zeng N, Du E, Guo Y, Peng C, He Y, Ma H (2014) Probing microstructural information of anisotropic scattering media using rotation-independent polarization parameters. Appl Opt 53(14):2949–2955
16. Bueno J, Cookson C, Kisilak M, Campbell M (2009) Enhancement of confocal microscopy images using Mueller-matrix polarimetry. J Microsc 235(1):84–93
17. Shi Y, McClain W, Harris R (1994) Generalized Stokes-Mueller formalism for two-photon absorption, frequency doubling, and hyper-Raman scattering. Phys Rev A 49(3):1999

18. Da Costa V, Wei R, Lim R, Sun C-H, Brown JJ, Wong BJ-F (2008) Nondestructive imaging of live human keloid and facial tissue using multiphoton microscopy. Arch Facial Plast Surg 10(1):38–43
19. Oldenbourg R, Török P (2000) Point-spread functions of a polarizing microscope equipped with high-numerical-aperture lenses. Appl Opt 39(34):6325–6331
20. Lu S-Y, Chipman RA (1996) Interpretation of Mueller matrices based on polar decomposition. JOSA A 13(5):1106–1113
21. Wood MF, Ghosh N, Wallenburg MA, Li S-H, Weisel RD, Wilson BC, Li R-K, Vitkin IA (2010) Polarization birefringence measurements for characterizing the myocardium, including healthy, infarcted, and stem-cell-regenerated tissues. J Biomed Opt 15(4):047009
22. Ghassemi P, Lemaillet P, Ramella-Roman JC, Shupp JW, Venna SS, Boisvert ME, Flanagan K, Jordan MH, Germer TA (2012) Out-of-plane Stokes imaging polarimeter for early skin cancer diagnosis. J Biomed Opt 17(7):076014
23. Adams DC, Hariri LP, Miller AJ, Wang Y, Cho JL, Villiger M, Holz JA, Szabari MV, Hamilos DL, Harris RS (2016) Birefringence microscopy platform for assessing airway smooth muscle structure and function *in vivo*. Sci Transl Med 8(359):359ra131–359ra131
24. Qi J, He H, Ma H, Elson DS (2017) Extended polar decomposition method of Mueller matrices for turbid media in reflection geometry. Opt Lett 42(20):4048–4051
25. Kumar MS, Simon R (1992) Characterization of Mueller matrices in polarization optics. Opt Commun 88(4–6):464–470
26. Simon B, Simon S, Mukunda N, Gori F, Santarsiero M, Borghi R, Simon R (2010) A complete characterization of pre-Mueller and Mueller matrices in polarization optics. JOSA A 27(2):188–199
27. Reddy SG, Prabhakar S, Chithrabhanu P, Singh R, Simon R (2016) Polarization state transformation using two quarter wave plates: application to Mueller polarimetry. Appl Opt 55(12):B14–B19
28. Mohanty SK, Ghosh N, Majumder SK, Gupta PK (2001) Depolarization of autofluorescence from malignant and normal human breast tissues. Appl Opt 40(7):1147–1154
29. Ellingsen PG, Aas LMS, Hagen VS, Kumar R, Lilledahl MB, Kildemo M (2014) Mueller matrix three-dimensional directional imaging of collagen fibers. J Biomed Opt 19(2):026002
30. Ghosh N, Wood MF, Li S, Weisel RD, Wilson BC, Li RK, Vitkin IA (2009) Mueller matrix decomposition for polarized light assessment of biological tissues. J Biophotonics 2(3):145–156
31. Qi J, Elson DS (2016) A high definition Mueller polarimetric endoscope for tissue characterisation. Sci Rep 6:25953
32. Wang Y, He H, Chang J, He C, Liu S, Li M, Zeng N, Wu J, Ma H (2016) Mueller matrix microscope: a quantitative tool to facilitate detections and fibrosis scorings of liver cirrhosis and cancer tissues. J Biomed Opt 21(7):071112
33. Wood MF, Ghosh N, Moriyama EH, Wilson BC, Vitkin IA (2009) Proof-of-principle demonstration of a Mueller matrix decomposition method for polarized light tissue characterization *in vivo*. J Biomed Opt 14(1):014029
34. Dong Y, Qi J, He H, He C, Liu S, Wu J, Elson DS, Ma H (2017) Quantitatively characterizing the microstructural features of breast ductal carcinoma tissues in different progression stages by Mueller matrix microscope. Biomed Opt Express 8(8):3643–3655
35. Ellingsen PG, Lilledahl MB, Aas LMS, de Lange Davies C, Kildemo M (2011) Quantitative characterization of articular cartilage using Mueller matrix imaging and multiphoton microscopy. J Biomed Opt 16(11):116002
36. Novikova T, Pierangelo A, Manhas S, Benali A, Validire P, Gayet B, De Martino A (2013) The origins of polarimetric image contrast between healthy and cancerous human colon tissue. Appl Phys Lett 102(24):241103
37. Antonelli M-R, Pierangelo A, Novikova T, Validire P, Benali A, Gayet B, De Martino A (2010) Mueller matrix imaging of human colon tissue for cancer diagnostics: how Monte Carlo modeling can help in the interpretation of experimental data. Opt Express 18(10): 10200–10208
38. Pierangelo A, Nazac A, Benali A, Validire P, Cohen H, Novikova T, Ibrahim BH, Manhas S, Fallet C, Antonelli M-R (2013) Polarimetric imaging of uterine cervix: a case study. Opt Express 21(12):14120–14130
39. Vizet J, Rehbinder J, Deby S, Roussel S, Nazac A, Soufan R, Genestie C, Haie-Meder C, Fernandez H, Moreau F (2017) *In vivo* imaging of uterine cervix with a Mueller polarimetric colposcope. Sci Rep 7(1):2471
40. Wang W, Lim LG, Srivastava S, Bok-Yan So J, Shabbir A, Liu Q (2016) Investigation on the potential of Mueller matrix imaging for digital staining. J Biophotonics 9(4):364–375
41. Pierangelo A, Benali A, Antonelli M-R, Novikova T, Validire P, Gayet B, De Martino A (2011) Ex-vivo characterization of human colon cancer by Mueller polarimetric imaging. Opt Express 19(2): 1582–1593
42. Dong Y, He H, Sheng W, Wu J, Ma H (2017) A quantitative and non-contact technique to characterise microstructural variations of skin tissues during photo-damaging process based on Mueller matrix polarimetry. Sci Rep 7
43. Ferlay J, Shin HR, Bray F, Forman D, Mathers C, Parkin DM (2010) Estimates of worldwide burden of cancer in 2008: GLOBOCAN 2008. Int J Cancer 127(12):2893–2917
44. Bancelin S, Nazac A, Ibrahim BH, Dokládal P, Decencière E, Teig B, Haddad H, Fernandez H, Schanne-Klein M-C, De Martino A (2014) Determination of collagen fiber orientation in histological slides using Mueller microscopy and validation by second harmonic generation imaging. Opt Express 22(19):22561–22574
45. Arifler D, Pavlova I, Gillenwater A, Richards-Kortum R (2007) Light scattering from collagen fiber networks: micro-optical properties of normal and neoplastic stroma. Biophys J 92(9):3260–3274
46. He H, He C, Chang J, Lv D, Wu J, Duan C, Zhou Q, Zeng N, He Y, Ma H (2017) Monitoring microstructural variations of fresh skeletal muscle tissues by Mueller matrix imaging. J Biophotonics 10(5): 664–673
47. Chen D, Zeng N, Xie Q, He H, Tuchin VV, Ma H (2017) Mueller matrix polarimetry for characterizing microstructural variation of nude mouse skin during tissue optical clearing. Biomed Opt Express 8(8):3559–3570
48. Kunnen B, Macdonald C, Doronin A, Jacques S, Eccles M, Meglinski I (2015) Application of circularly polarized light for non-invasive diagnosis of cancerous tissues and turbid tissue-like scattering media. J Biophotonics 8(4):317–323
49. Aas LMS, Ellingsen PG, Kildemo M (2011) Near infra-red Mueller matrix imaging system and application to retardance imaging of strain. Thin Solid Films 519(9):2737–2741
50. Golaraei A, Kontenis L, Cisek R, Tokarz D, Done SJ, Wilson BC, Barzda V (2016) Changes of collagen ultrastructure in breast cancer tissue determined by second-harmonic generation double Stokes-Mueller polarimetric microscopy. Biomed Opt Express 7(10): 4054–4068